processes

MDPI

Article

A cleaner delignification of urban leaf waste biomass for bioethanol production, optimized by experimental design

Gustavo Kildegaard [1], María del Pilar Balbi [1], Gabriel Salierno [1,2,3,*], Miryan Cassanello [1,2], Cataldo De Blasio [3], and Miguel Galvagno [4]

[1] Universidad de Buenos Aires, Facultad de Ciencias Exactas y Naturales, Dpto. Industrias, LARSI, Ciudad Universitaria, C1428BGA, Buenos Aires, Argentina. E-mail: miryan@di.fcen.uba.ar
[2] CONICET, Universidad de Buenos Aires, Instituto de Tecnología de Alimentos y Procesos Químicos (ITAPROQ), Facultad de Ciencias Exactas y Naturales, C1428BGA, Buenos Aires, Argentina
[3] Åbo Akademi University, Faculty of Science and Engineering, Energy Technology. Rantakatu 2, 65100 Vaasa. Finland. E-mail: cdeblasi@abo.fi
[4] Instituto de Investigaciones Biotecnológicas (IIBio), UNSAM-CONICET. B1650HMP, Buenos Aires, Argentina. E-mail: miguelgalvagno@gmail.com
* Correspondence: gabriel.salierno@gmail.com ; gabriel.salierno@abo.fi

Abstract: This work presents a study of the conditions leading to improved delignification of urban forest waste typical of Buenos Aires. Particularly, the leaf waste of *Platanus acerifolia* has been studied. Delignification was accomplished by acid-oxidative digestion using acetic acid and 30% hydrogen peroxide 1:1. The effect of reaction time (30–90 min), temperature (60–90 °C), and solid loading (5–15 g solid/20g liquid) on delignification and solid fraction yield were studied. The process parameters were optimized using the Box-Behnken experimental design. The highest attained lignin removal efficiency was larger than 80%. The optimized conditions of delignification, while maximizing holocellulose yield, pointed to using the minimum temperature of the examined range. Analysis of variance on the solid fraction yield and the lignin removal suggested a linear model with a negative influence of the temperature on the yield. Furthermore, a negative effect of the solid loading and low effect of temperature and time was found on the degree of delignification. Then the temperature range was extended back to 60°C, and good results both of yield and delignification were obtained. Significant delignification with good yield attained at moderate temperature. Lignin removal was visualized using confocal laser scanning microscopy. The solid structure was slightly modified as judged from scanning electron microscopy.

Keywords: Biomass delignification; acid-oxidative hydrolysis; experimental design; urban waste

Citation: Lastname, F.; Lastname, F.; Lastname, F. Title. *Processes* **2022**, *10*, x. https://doi.org/10.3390/xxxxx

Academic Editor: Firstname Lastname

Received: date
Accepted: date
Published: date

1. Introduction

The urgency of accelerating development in a sustainable direction within a context of social demand for practices in compliance with standards of minimum environmental impact is reflected in the prerequisite for existing processes intensification and reduced risks of scaling up novel cleaner energy technologies based on renewable raw materials [1] while ensuring the continuity of energy supply. In this context, biomass is fundamental to a future energy sector adaptation and effectively mitigates climate change since energy production is the main source of carbon emissions [2]. Biofuels are crucial for reducing fossil-fuel dependency and greenhouse gas emissions. Bioethanol is a promising sustainable candidate for substituting gasoline [3]. Ethanol utilization in the world is available up to 20% blend in gas fuels.

Cellulosic ethanol presents an exciting and tangible but underdeveloped economic opportunity for ethanol producers, as the fuel's greater greenhouse gas (GHG) reductions

[4]. Most of the produced bioethanol is considered a first-generation biofuel because the raw material for the process is starch or glucose, coming mainly from the arable land for food production [5]. The major negative social impact of first-generation bioethanol production can be sorted by using Lignocellulosic Biomass as starting material because of effective decoupling with food production. The limitation of the so-called second-generation bioethanol is mainly the relatively low bioavailability of glucose of the feedstock because of the presence of lignin [6], which hinders yield, and it is considered a low-value residue. Many second-generation bioethanol industrial initiatives could fail if the technology gaps are not carefully addressed. A third of the bioethanol world supply was predicted to be produced in 2020, parting from LCW [7], but currently and unfortunately, less than 2% of the market is supplied by this methodology [8]. Most pilot experiences all over the world were unsuccessful at scaling up. Unit integration and system optimization are the ultimate solutions for making the cellulosic ethanol production process [9].

Conversion of agro-industrial and urban wastes (lignocellulosic wastes – LCW) to energy is an innovative approach for waste valorization and management, simultaneously mitigating environmental pollution. Utilizing LCW has economic benefits while addressing the issue of food vs. fuel controversy, being an attractive alternative for disposal of agricultural, forestry, and urban waste [10–14]. Garden and street forest waste is an important lignocellulosic feedstock recognized as a resource [15]. Besides conventional processing methods like burial, microbial composting, and biochar production, biorefineries to produce biogas and bioethanol from garden and forestry waste have attracted global attention [16–19]. In Buenos Aires city, with streets beautifully covered by trees, this type of waste can reach hundreds of tons per day. Although they are partially treated in a city's recycling plant [20] and used for compost and pulping, specific information for optimizing this LCW valorization is relevant for intensifying and diversifying the processes.

There are four basic processes involved in the biochemical production and obtaining of ethanol by yeasts from cellulosic biomass: pretreatment for cellulose separation from lignin (called delignification), enzymatic hydrolysis of cellulose (called saccharification), fermentation, and distillation. The optimization of delignification and saccharification are key to improving fermentation efficiency. The pretreatment of LCW is a key stage to disrupt the recalcitrant structure of lignocellulose [10]. The delignification processes traditionally used in the extraction of cellulose for paper production and the methods that use strong acids and alkalis are not adequate to generate a bioavailable substrate for fermentation [21]. Classical dilute acid pretreatments require high temperatures and the remaining lignin still hinders access to the cellulose fibers [17]. Delignification of LCW strongly facilitates the hydrolysis of holocellulose to fermentable sugars involved in producing biofuels and other bio-based chemicals.

Moreover, at high temperatures, aliphatic acids, and furans toxic for fermenting microorganisms are formed [10,22–24]. Therefore, developing low-temperature pretreatments is important to reduce toxic molecules and energy consumption. The high oxidative mixture of hydrogen peroxide and acetic acid has been suggested as a low-temperature pretreatment with high lignin removal efficiency, leading to significant recovery of fermentable sugars [25–27]. The PoxAc delignification process [27] is based on a mixture of hydrogen peroxide in glacial acetic acid, which allows cellulose to be separated and obtaining high-quality lignin to be used in a variety of applications, such as Supercritical Water Gasification to produce hydrogen [28] and materials for 3D printing [29]. The PoxAc delignification method uses reagents that decompose into harmless compounds produces a substrate that allows better productivity of sugars through enzymatic and biological treatments. In addition, delignified LCW can be used for other purposes, such as fluid rheology modifiers [30], as reinforcement material in composites and biodegradable polymers, as strength additives in textile printing and coating products [31,32], and many more.

Platanus acerifolia is widely planted in major cities since it is a tough, durable tree that can tolerate severe pruning and smog. The plant typically grows up to 25 m and has a good shading capacity for dense leaf. This species is frequently found in many neighborhoods around the city of Buenos Aires. Hence, this work aims at examining and optimizing conditions to attain delignification of the leaf waste arising from the street sweeping of this species. For this purpose, the low-temperature acid-oxidative hydrolysis of the LCW is accomplished by digestion in a solution of glacial acetic acid and 30% hydrogen peroxide 1:1 (v/v) ratio, which was suggested as the best proportion for delignification [27].

2. Materials and Methods

2.1. Raw material pretreatment and characterization

The leaf waste was obtained from the leaves sweeping a street in the Saavedra neighborhood within Buenos Aires, where all the planted trees were *Platanus acerifolia*. The material (6kg) was separated from dust in an industrial sieve, mainly retaining dry leaves and stems. Then, the LCW was humidified, added to the same water mass, and triturated in batches of 1kg using a 2200W Turbo blender at 35000 rpm for 10 minutes. The resulting LCW was homogenized and kept in a freezer for subsequent characterization and a series of experiments. Analytical grade hydrogen peroxide, acetic acid, and sulphuric acid were used for the experiments.

The moisture of the samples was determined using a Precisa XM50 moisture analyzer (Precisa Gravimetrics AG, Dietikon, Switzerland). Standard methods determined the ash content and ethanol extractives. Lignin acid-insoluble contents of the untreated and treated samples were determined by dissolving 0.3 g of the specific substrate with 4mL of 72% v/v sulphuric acid and let to react 3 hours at room temperature (28ºC). Then, the solution was diluted to 5% v/v (1M) with distilled water and heated to 100ºC for 2.5 hours. The suspension was filtrated, dried, and weighted. The lignin content is obtained as the final dry mass referred to the initial solid dry mass. The cellulose content of the untreated sample was determined by dissolving 0.3 g of the substrate into 4mL of 72% v/v sulphuric acid. Immediately afterward, the solution was diluted to 5% v/v (1M) with distilled water, and the hydrolysis proceeded by heating to 100ºC for 2.5 hours. The suspension was filtrated, dried, and weighted. The cellulose content was determined as the difference between final and initial dry masses [33,34].

The oxidative hydrolysis was carried out in batch mode in 100mL Erlenmeyer, with orbital shaking. A solution (20 mL) containing equivalent volumes of glacial acetic acid and 30% hydrogen peroxide was contacted with different masses of LCW (5 to 15 g). The orbital shaker allowed regulating temperature and time. The temperature was modified within the 60-90°C range, while digestion was varied between 30 and 90 minutes. For reference, one sample was treated with a dilute solution of sulfuric acid (0.1M) under the conditions (90min, 90°C, 5g) that were found as optimal for biomass pretreatment aimed at subsequent enzymatic saccharification for bioethanol production [35]. The treated samples were filtered from the acid-oxidant liquor with a cheesecloth. Moisture and lignin content of the obtained solid samples were determined to get the solid fraction yield and lignin removal efficiency, as expressed in Eqs. 1 and 2, were m_0^{dry} and m_f^{dry} are the initial and final mass of solid samples on a dry and ash-free basis, and $\%Lignin$ indicates the fraction of insoluble lignin in the dry and ash-free basis.

$$\text{Solid fraction yield} = \frac{m_f^{dry}}{m_0^{dry}} \quad (1)$$

$$\text{Lignin removal} = \frac{\%Lignin_0 m_0^{dry} - \%Lignin_f m_f^{dry}}{\%Lignin_0 m_0^{dry}} \quad (2)$$

For data analysis, the so-called severity factor, Ro, defined as in Eq. (3) was considered, where "t" represents the digestion time in minutes, "T" is the treatment temperature in °C, and "T_{ref}" is 100 °C, a reference temperature [12,22].

$$\text{Severity factor } \text{Ro} = \text{t} \cdot exp\left(\frac{\text{T} - \text{T}_{\text{ref}}}{14.75}\right) \quad (3)$$

2.2. Confocal Laser Scanning Microscopy (CLSM)

Variations of the lignin content between treated and untreated samples were assessed by CLSM, discriminating the leaves and stems portions of the LCW. Under the conditions used to observe the samples, lignin exhibits autofluorescence and can be easily distinguished by this technique from other components without contrast reagents [36–38]. The images were obtained using an Olympus FV300/BX61 confocal microscope (Olympus, Japan). The samples were first dried, fixed on glass slides, and covered with a thin glass lid. They were first observed under an optical microscope (UPLFL 10X). After establishing the proper focus, multiple stacks of 1024p x 1024p pictures were taken with laser excitation at 405nm and fluorescence emission detection at 550nm, characteristic of lignin, in scanning mode [36]. Magnification was at 10X as well as an objective lens (UPLFL 10X). Images were analyzed using the ImageJ open-source software (https://imagej.nih.gov/). The stack was averaged over the Z-axis and converted to a 0-255 grayscale (8-bit). Mean intensity was calculated from these images averaging all pixels of the best-focused image, as suggested by Hernández-Hernández et al. (2016, 2014) [38,39].

2.3. Scanning electron microscopy (SEM)

Changes in surface morphology of untreated and delignified samples were examined under scanning electron microscope Carl Zeiss NTS-Supra 40 (Carl Zeiss AG, Oberkochen, Germany). Before analysis, the samples were fixed on the sample plates using carbon tape as a non-conducting adhesive. Then, the samples were subjected to gold sputtering to increase their conductivity before taking the micrographs.

3. Experimental design

The acid-oxidative hydrolysis of the LCW is a multivariable process in which the variables interact with one another. Therefore, experimental design techniques present a more balanced alternative to the *ceteris paribus* (i.e., one variable at a time) approach to obtain information and improve the conditions for the delignification stage with good holocellulose yield [40–42]. The Statistical Design of Experiments (DoE) combined with the Response Surface Methodology (RSM) analysis covers only a fraction of the experimental space. The DoE-RSM method allows drawing effective conclusions while estimating the interactions between the different variables. Methods for experimental design can be broadly divided into two categories:

i) One includes designs used to explore a potentially large number of input variables to discover those that are statistically significant and estimate their magnitude. Plackett-Burman (PBSD) and Factorial Fractional designs are examples of these methods [42].

ii) The other category includes methods for optimizing a process given a reduced number of variables selected previously. A typical scenario is Central Composite (CC) or Box Behnken Design (BBD) and a RSM analysis on linear or quadratic models. Moreover, RSM analysis allows fine-tuning of any process variables, an issue to be considered when an industrial scale is aimed [42]. The objectives of the

RSM are to confirm observed or assumed effects in the variable selection stage and quantify the most appropriate values for the parameters under study to optimize the response. Finally, the predicted optimum must be verified after model building and optimization.

3.1. Box Behnken Design of Experiment

Box Behnken DoE aims to find the effects of factors, estimate the curvature or quadratic effects, and determine the most appropriate values for the parameters under study to find the response surface and minimize the required set of experiments. The influences of solid loading, acid-oxidative hydrolysis temperature, and time on delignification efficiency and solid fraction yield were evaluated using full factorial design in Minitab 17 software. Mathematical matrices will be constructed within the ranges of the chosen variables. The three independent variables have three levels (-1, 0, and +1; **Table 1**) and three central points, leading to 15 combinations (**Table 2**). The severity factor calculated from the time and temperature conditions is included in **Table 2**. Apart from the combinations arising from the Box & Behnken Design, the hydrolysis conditions with sulfuric acid were carried out for comparison. The experiments carried out to extend the analysis of the temperature influence are indicated in **Table 2**.

Table 1: Levels of factors tested in the Box and Behnken Design of Experiments for optimizing LCW delignification.

Factors	**Levels**		
	-1	0	1
Time (min)	30	60	90
Temperature (°C)	70	80	90
Solid Loading (g/ 20mL liquid)	5	10	15

209

Table 2: Factor combinations considered for the Box & Behnken Design. 210

Run	Time (min)	Temperature (°C)	Solid Loading (g/20mL liquid)	Log (Ro)
1	90	80	15	1.37
2	30	80	15	0.89
3	90	70	10	1.07
4	60	90	5	1.48
5	90	80	5	1.37
6	60	70	15	0.89
7	90	90	10	1.66
8	60	80	10	1.19
9	60	80	10	1.19
10	30	70	10	0.59
11	60	70	5	0.89
12	30	80	5	0.89
13	30	90	10	1.18
14	60	90	15	1.48
15	60	80	10	1.19
S1	90	90	5	1.66
E1	60	60	5	0.60

211

4. Results and discussion

4.1. Effect of the acid-oxidative hydrolysis on the LCW characteristics

The proximal composition of the *Platanus acerifolia* leaf waste was studied to evaluate their potential for biofuel or biochemical production. LCW moisture was evaluated every time it was used for experiments to assess the exact solid dry mass. Moisture was always around 70% w/w. The dry leaf waste contained a minor amount of ash (3.2% w/w) and ethanol extractives (4% w/w), significant insoluble lignin (44% w/w), cellulose (12% w/w), and hemicellulose (36% w/w). After the hydrolysis, moisture and lignin content were determined to get the solid fraction yield and % delignification. **Figure 1** illustrates a photograph of the untreated sample and samples treated with dilute sulphuric acid (Run #S1, **Table 2**) and the acid-oxidative hydrolysis (Runs #6, #7, #11, and #E1, **Table 2**). There is a significant difference in the color of the sample, which correlates with the lignin content. Still, the appearance of the pre-treated leaf waste is similar to the untreated sample.

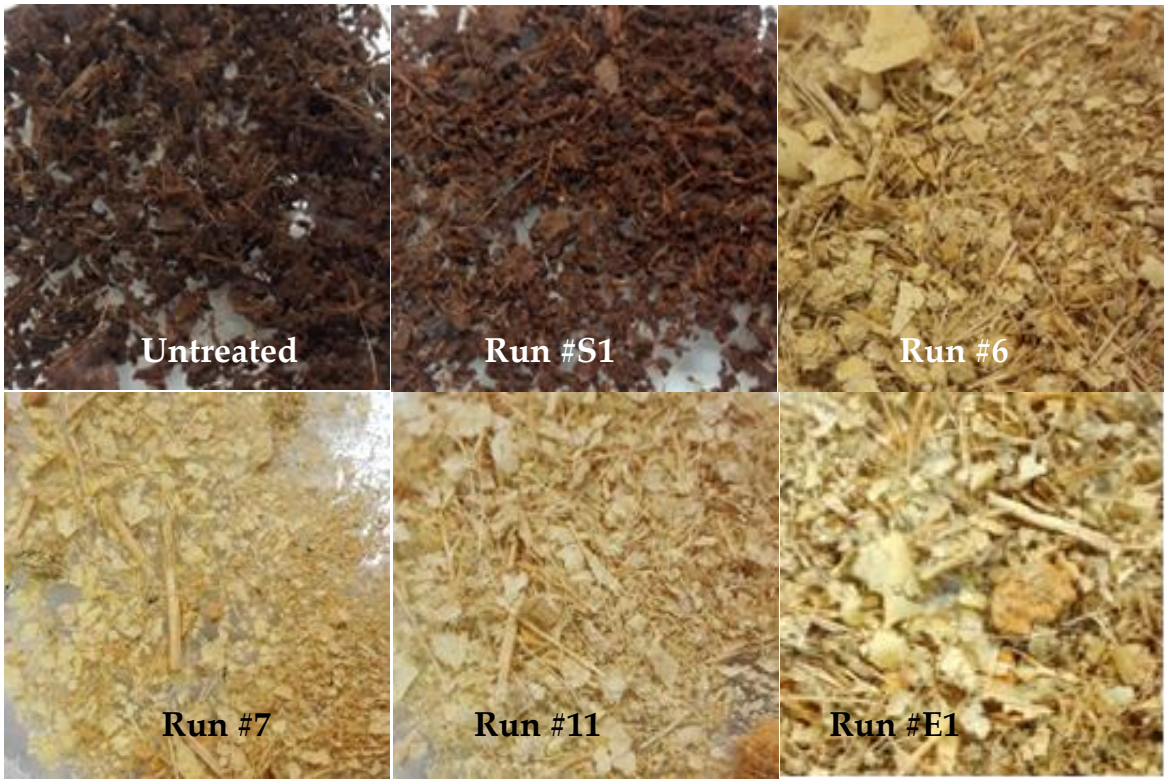

Figure 1: Photograph of the untreated LCW, the LCW pre-treated with a dilute sulphuric acid solution (Run #S1-Table 2), and the LCW pre-treated by the acid-oxidative hydrolysis at conditions of Run #6, #7, #11, and E1.

Attaining a high solid fraction with the acid-oxidative hydrolysis pretreatment since the carbohydrates usable for bioprocess remain in the solid. The solid fraction decreased as the severity increased (**Figure 2**), mainly related to the temperature effect. The yield has an almost linear negative dependence on the severity factor, particularly for the lowest solid loading. On the contrary, the effect of the severity factor on the delignification efficiency (**Figure 3**) is slightly positive, and an influence of the solid loading is perceived. Despite significant variations, the attained delignification was always larger than 60% except for one condition corresponding to the highest solid loading examined. The highest delignification degree was attained for the lowest examined solid loading, reaching a value of 85.2% for Run #4 of **Table 2**, although solid yield for this condition was less than 50%.

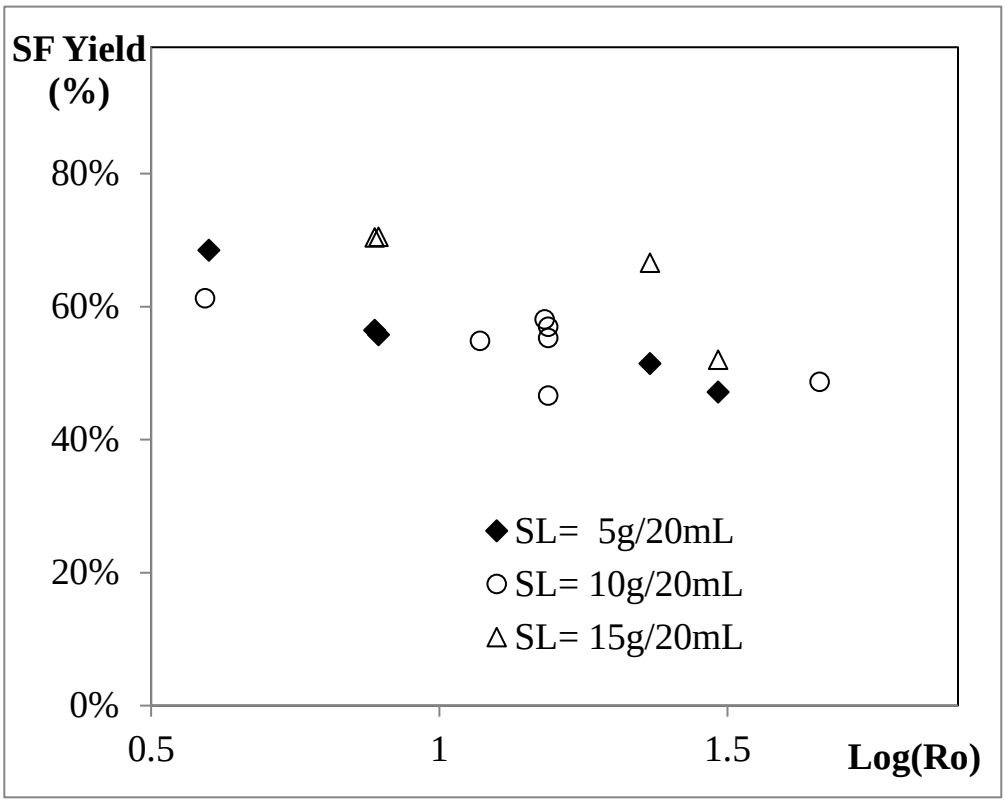

Figure 2: Effect of the severity factor on the solid fraction yield.

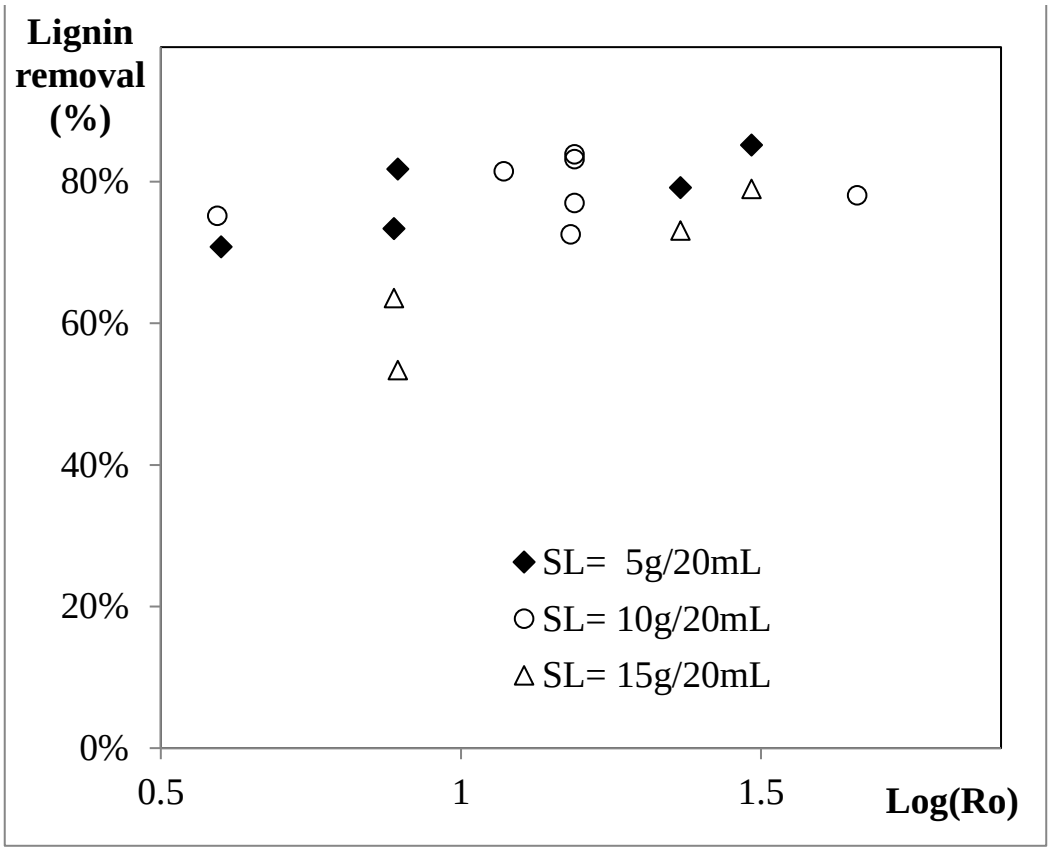

Figure 3: Effect of the severity factor on the delignification efficiency.

4.2. CLSM autofluorescence imaging

Error! Reference source not found. and **Error! Reference source not found.** show micrographs are highlighting the lignin autofluorescence (in green) of the samples before and after the acid-oxidative hydrolysis, keeping the same laser excitation intensity, optical augmentation, and scan rate.

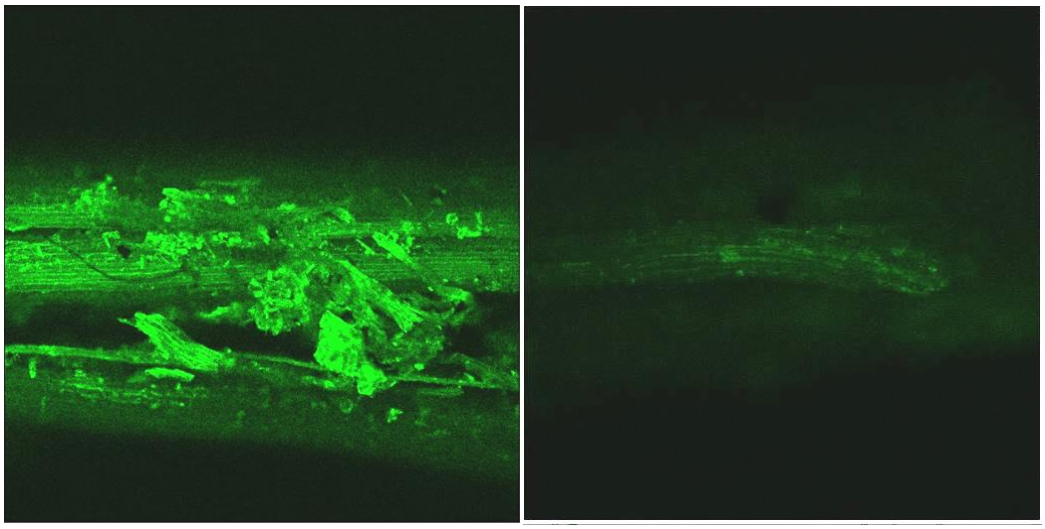

Figure 4. CLSM taken from the portion containing stems of the untreated sample (left) and the sample after the oxidative hydrolysis under conditions of Run #4 (right).

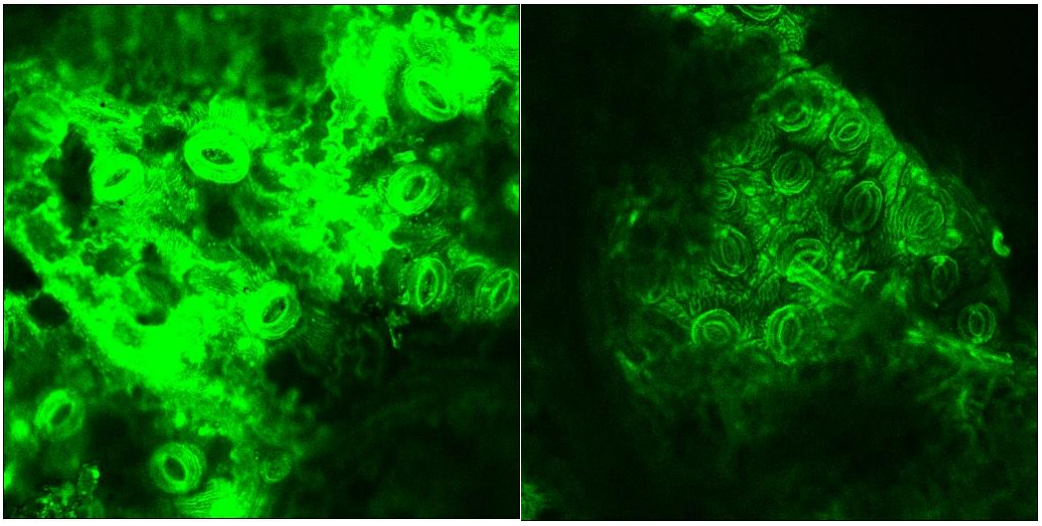

Figure 5. CLSM taken from a portion of the untreated leaf sample (left) and the sample after the oxidative hydrolysis under Run #4 (right) conditions.

A significant reduction of the lignin autofluorescence intensity is observed in the treated samples compared to the original, both in the leaves and stems portions of the LCW. **Error! Reference source not found.** shows details of a stoma from the nerve side of the leaves before and after treatment illustrating that the lignin content is high in the stomata region and largely removed by the treatment.

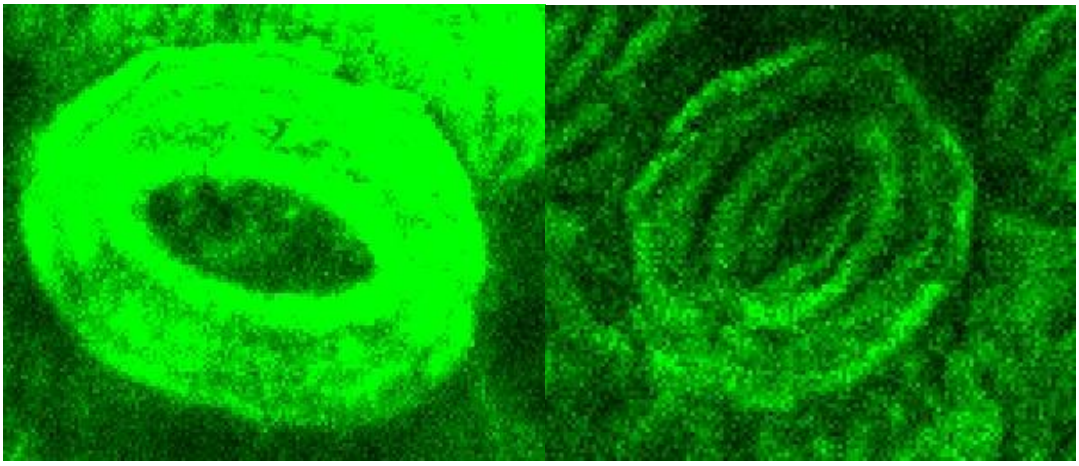

Figure 6. CLSM of a stoma from a portion of the untreated leaf sample (left) and the sample after the oxidative hydrolysis under conditions of Run #4 (right).

Images were taken for the untreated sample and obtained after runs #4, #6, and #S1.

Mean fluorescence intensity was estimated from the images using the ImageJ software by averaging over the Z-axis converted to a 0-255 grayscale (8-bit). It was found that the mean intensity correlated well with the amount of lignin in the sample (**Error! Reference source not found.**). The fluorescence intensity of the samples decreased after the acid-oxidative hydrolysis, proportional to the severity factor. However, despite having the highest severity factor, the sample treated with sulphuric acid showed the highest lignin content and fluorescence intensity, indicating the low degree of delignification and partial dissolution of cellulose.

Table 3. Autofluorescence intensity as a function of the treatment severity.

Sample	Log (Ro)	% Lignin	Fluorescence Intensity
Untreated	-	40%	++++
Run #6	0.89	28%	++
Run #4	1.48	14%	+
Run S1	1.66	45%	+++

4.3. SEM imaging

The surface morphological characteristics of the untreated and treated LCW samples were analyzed by SEM, and representative results are presented in **Figure 4** and **Error! Reference source not found.**. Leaves and stems structures have been observed in the SEM of the untreated sample (**Figure 4**). Stomata with guard cells are observed in the leaves (**Figure 4** a-b), as previously reported (Pourkhabbaz et al., 2010). The untreated leaf samples exhibited a compact, non-porous, uniform appearance of surface structure. In contrast, the stems presented porous longitudinal arrangement of fibrils (**Figure 4** c-d), as observed for other LCW (Hernández-Hernández et al., 2014).

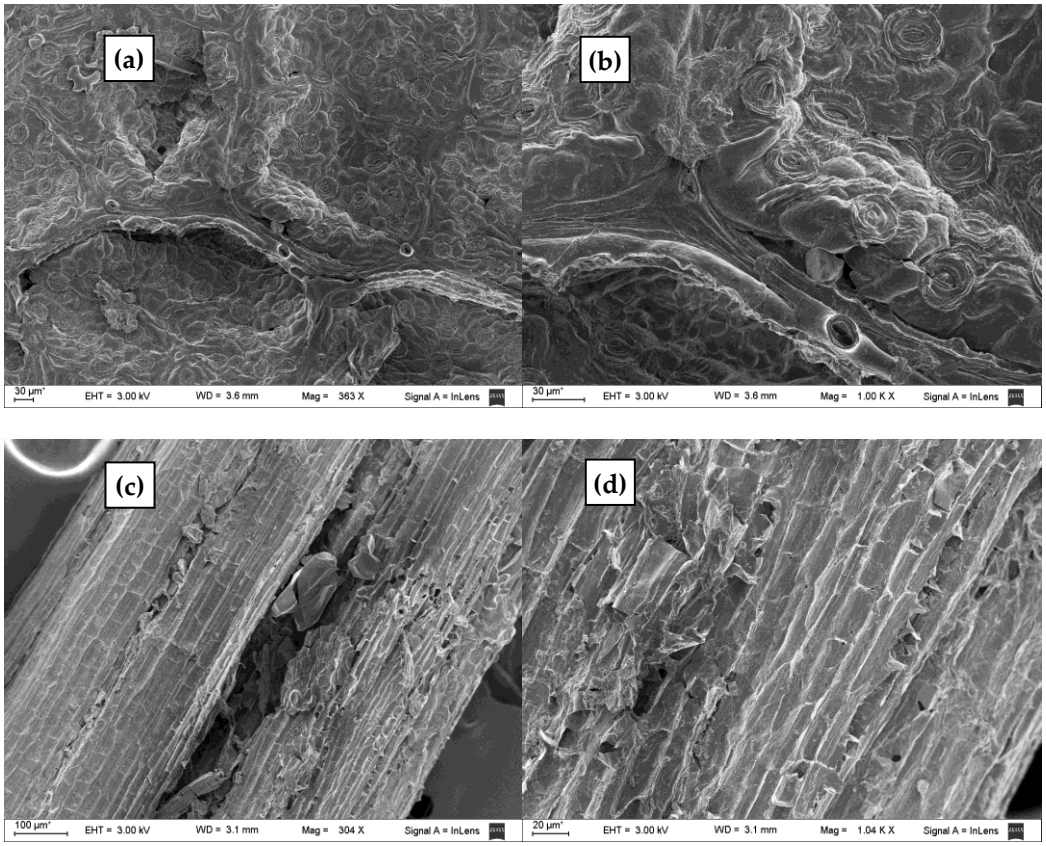

Figure 4: SEM photographs of (a-b) untreated leaves stomata and (c-d) untreated stems.

Enlargements of stomata untreated and treated with the acid-oxidative solution and with dilute sulphuric acid are illustrated in **Error! Reference source not found.** for comparison. The stomata structures were preserved after the treatments. However, the untreated surface (**Error! Reference source not found.**a) was apparently filled and covered by lignin, as confirmed by CLSM. The sample treated with sulphuric acid (**Error! Reference source not found.**b), with negligible delignification, appeared very similar to the untreated sample. Physical alterations of surface morphology observed in the samples treated with the acid-oxidative method for which lines are more defined and less uniform (**Error! Reference source not found.**c-d) could be due to lignin removal. SEM images revealed that the treatment further exposed cellulose fibers by dissolving the covering lignin, turning the substrates rougher. Even though the cellulose fiber structure was exposed, the polymer structure was kept suggesting that the hydrolysis to develop reducing sugars may require tough conditions.

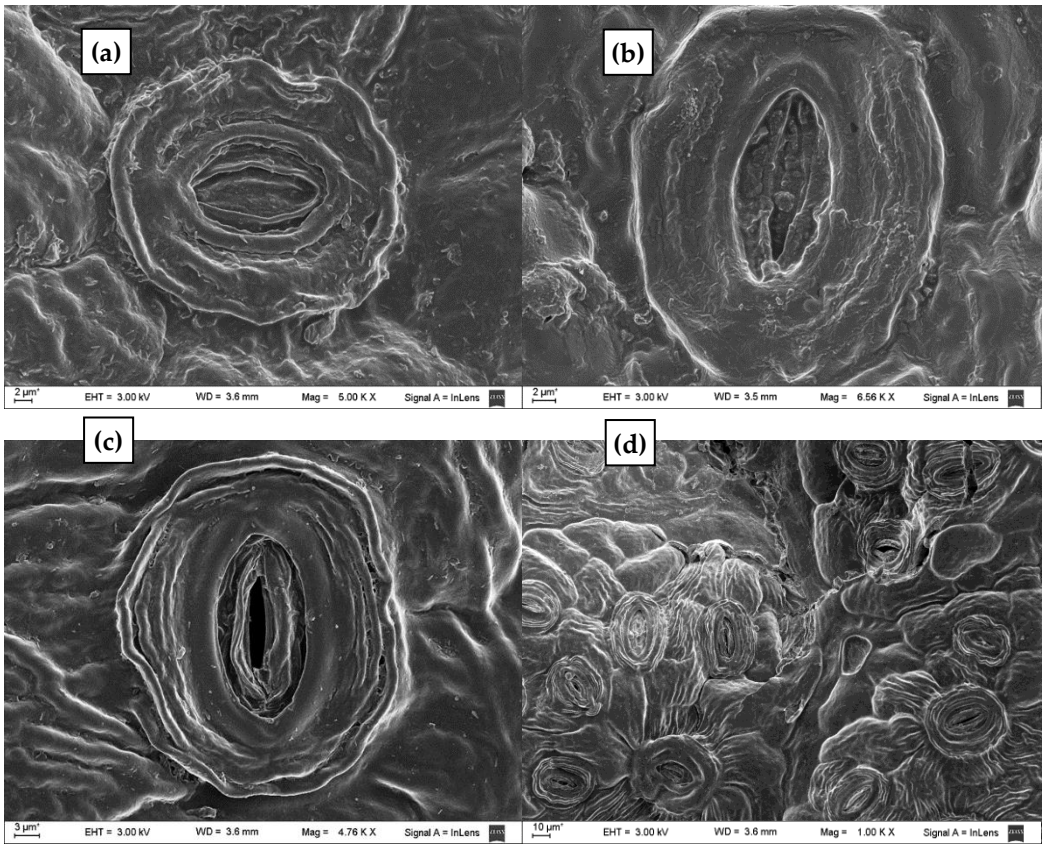

Figure 8. SEM photographs of: (a) untreated leaf stoma; (b) leaf stoma of a sample digested with a dilute solution of sulphuric acid at T = 90°, t = 90 min using 5 g solid/ 20 mL liquid ratio; (c-d) leaf stomata of a sample digested at T = 90°, t = 90 min using 10 g solid/ 20 mL liquid ratio.

4.4. Pretreatment performance response surface regression

The results obtained from the pretreatment DoE were analyzed based on RSM. A polynomial quadratic regression equation was obtained, representing the effect of independent factors and their interactions towards the output (solid fraction yield or % delignification). The interactive effects of parameters were analyzed based on 3D response surface plots. Each response was tested for a suitable best-fitting model. Analysis of variance (ANOVA) was done for the model terms (**Table 3**). The measured responses will be subjected to multiple least squares regression analysis. The student's t-test is used to evaluate statistical significance. Fischer's F test weights the adequacy of the mathematical regression model.

Interpretation of the parametric interaction of hemicellulose yield and lignin removal was evaluated as a combined effect of the three factors: time, temperature, and solid loading. Analysis of variance indicated a satisfactory linear model fit the solid fraction yield, with significant influence on the temperature and solid loading (**Table 3**). Maximum yields were attained for lower temperatures and the highest solid loadings (**Figure 5**).

Delignification was not well predicted by a linear or a single quadratic model; the best fit with a full quadratic model led to an R square of 76%. The analysis of variance indicated a significant influence of the solid loading and the temperature-solid loading interaction. As observed in **Figure 6**, the effect of solid loading on delignification is negative, interpretable mainly by the stoichiometry of the reaction between the oxidant

hydrogen peroxide and the lignin, which must be largely deconstructed to be extracted. However, the solid loading variable has a significant positive influence on the solid yield, which should be considered since the solid contains fermentable sugars. Temperature influence depends on the solid loading; it slightly affects the lowest solid loading. The optimum temperature found within the operation range can be interpreted as a compromise relationship between the severity factor and the thermal decomposition reaction of hydrogen peroxide, which competes with lignin oxidation. The hydrolysis time did not significantly modify the results; however, the surface response suggested that 60 min hydrolysis would provide better delignification.

Table 3: ANOVA of the RSM analysis for the solid fraction yield.

Response Surface Regression					
SF Yield (%) vs time (min), Temperature (°C) and Solid loading (g/mL)					
Analysis of Variance					
Source	**DF**	**Adj SS**	**Adj MS**	**F-Value**	**P-Value**
Model	9	0.0795	0.0088	3.46	0.092
Linear	3	0.0619	0.0206	8.09	0.023 – S
time (min)	1	0.0075	0.0075	2.95	0.146
Temperature (°C)	1	0.0199	0.0199	7.79	0.038 - S
Solid loading (g/mL)	1	0.0345	0.0345	13.52	0.014 – S
Square	3	0.0127	0.0042	1.66	0.289
time (min)*time (min)	1	0.0042	0.0042	1.66	0.253
Temperature (°C)×Temperature (°C)	1	0.0001	0.0001	0.06	0.820
Solid load (g/mL)×Solid load (g/mL)	1	0.0088	0.0088	3.44	0.123
2-Way Interaction	3	0.0049	0.0016	0.64	0.619
time (min)*Temperature (°C)	1	0.00023	0.00023	0.09	0.777
time (min)*Solid loading (g/mL)	1	0.00004	0.00004	0.01	0.911
Temperature (°C)×Solid load (g/mL)	1	0.00467	0.00467	1.83	0.234
Error	5	0.01276	0.00255		
Lack-of-Fit	3	0.00662	0.00220	0.72	0.627
Pure Error	2	0.006140	0.003070		
Total	14	0.092289			
Model Summary: S = 0.0505086 R-sq = 86.18%					

Given these results, the effect of decreasing the temperature to analyze the effect on delignification and solid fraction yield was studied further. A different experiment was carried out at 60°C, which provided a good yield (70%) and a good degree of delignification (71%). Under these conditions, the decrease in solid yield is occasioned mostly by lignin removal, optimal for recovering the fermentable sugars from the solid.

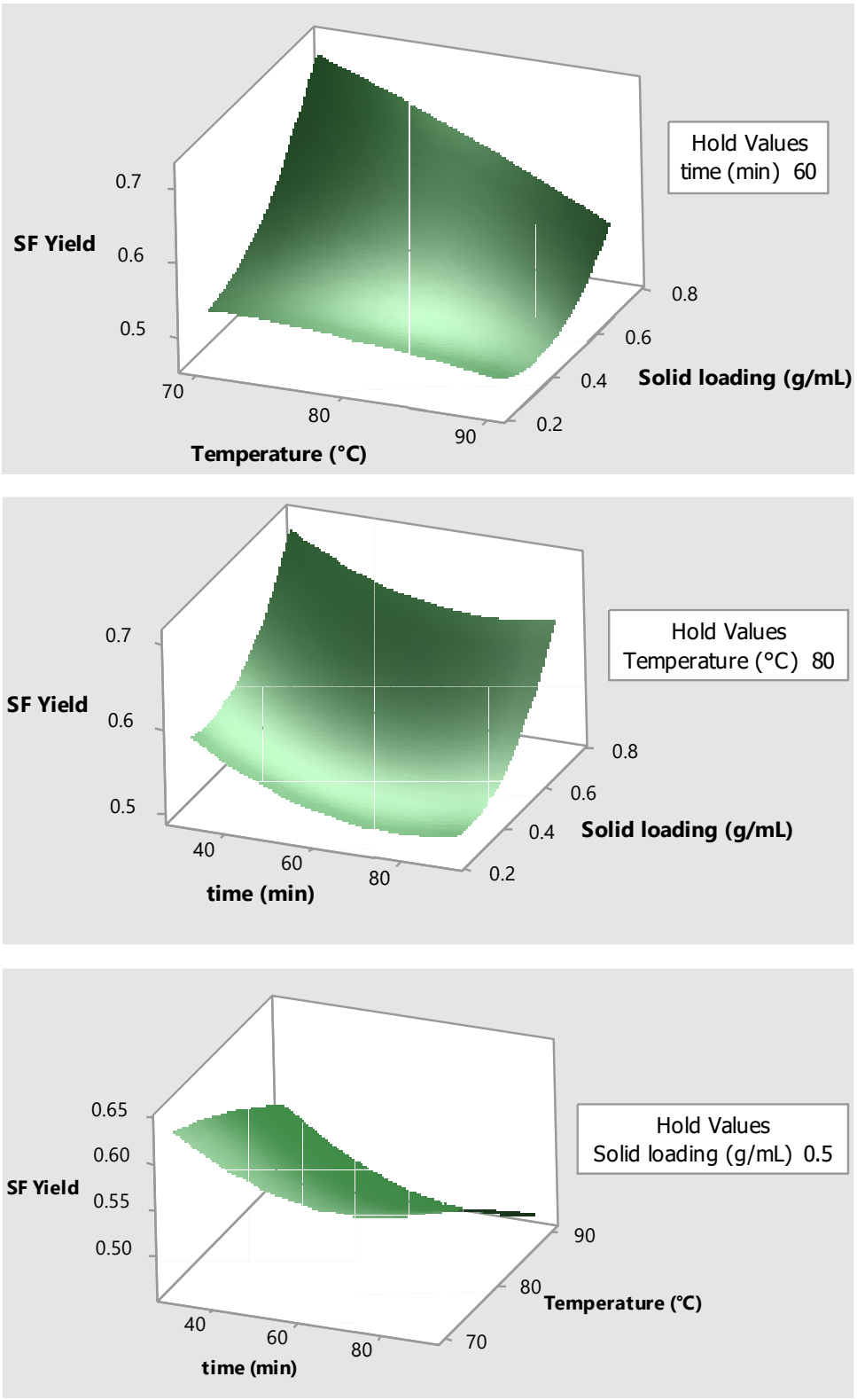

Figure 5: Surface plots of the solid fraction yield (Eq. 1) vs. solid loading, temperature, and time

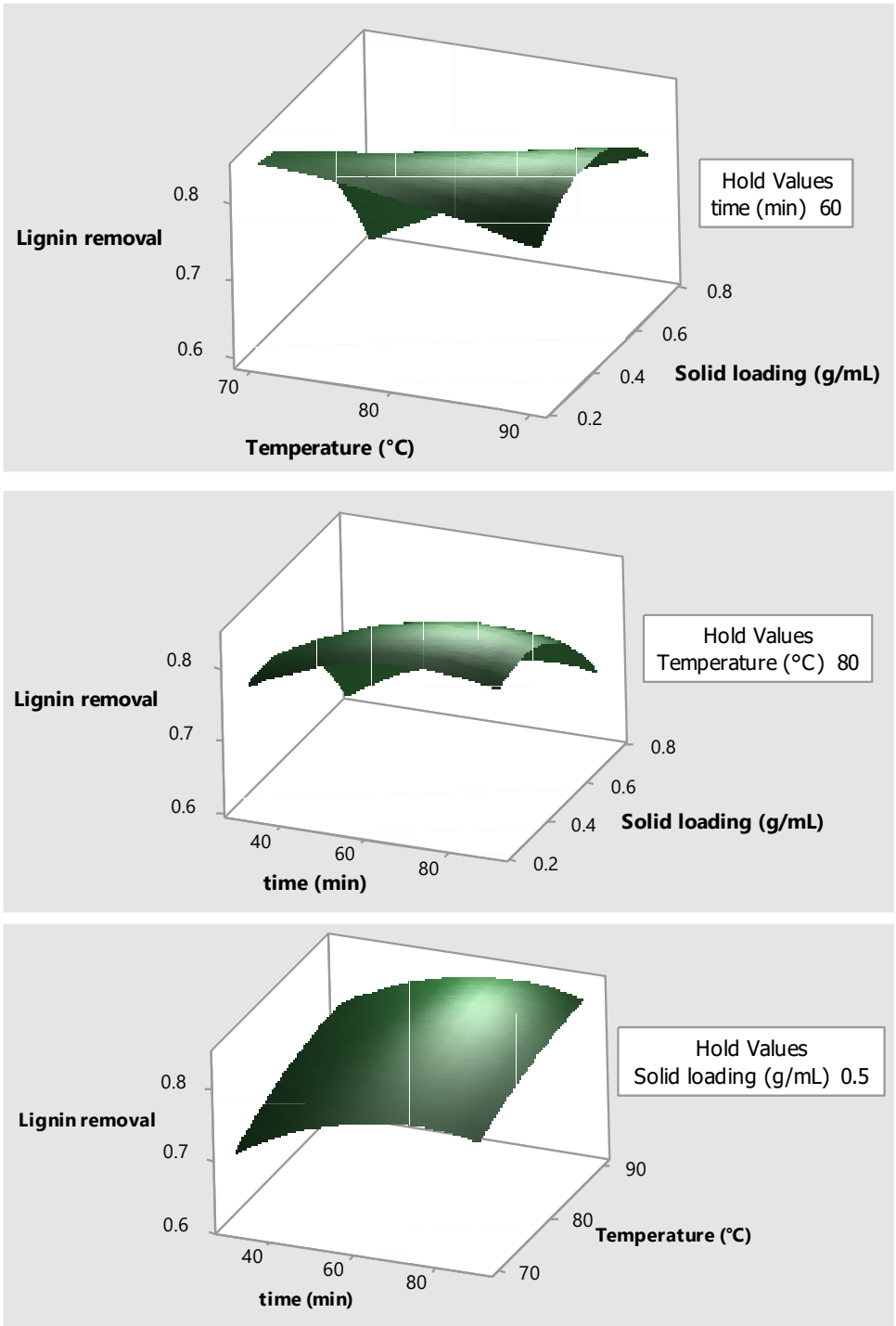

Figure 6: Surface plots of the lignin removal (Eq. 2) vs. the three factors considered

5. Conclusions

The effect of low-temperature acid-oxidative digestion on the delignification of urban forest leaf waste typical of parks and streets of Buenos Aires city was investigated. It was formed by swept *Platanus acerifolia* leaves and stemmed since it is widely planted in major cities. The experimental design was used to interpret the parametric interaction among the examined factors (time, temperature, and solid loading). Box and Behnken design of experiments successfully provided an acceptable surface model that could predict the behavior of further experiments, even outside the initial parameter range. The degree of delignification had a significant negative influence on the solid loading. Within the examined

conditions, the highest attained lignin removal was larger than 80%. Even if the temperature positively influences lignin removal, it negatively affects the solid fraction yield, mainly containing the remaining cellulose and hemicellulose fractions, eventually leading to the fermentable sugars usable for subsequent bioprocesses. Decreasing the hydrolysis temperature to 60°C led to 71% delignification and 70% solid yield, which are not far from those predicted as optimal by the models considered in this work. Confocal laser scanning microscopy confirmed the delignification of the samples by a significant decrease in the characteristic autofluorescence of lignin. Scanning electron microscopy analysis of the samples indicated better exposition of the cellulose fiber structure. The polymer structure was mainly conserved, suggesting that the hydrolysis to develop reducing sugars may require tough conditions.

Data Availability Statement: All data have been exposed in the article or are available upon request.

Author Contributions: G.K. & M.P.B: Investigation, experimental data acquisition, data curation; GS: data curation, formal analysis, writing and visualization; M.C.: Conceptualization, experimental design, writing original draft, supervision, funding acquisition; C.D.B: Consultation, review, and editing; M.G.: Conceptualization, experimental design, consultation, funding acquisition.

Funding: The authors gratefully acknowledge the financial support from Universidad de Buenos Aires (UBACyT 20020170100604BA), UNSAM, CONICET (PIP 1122015-0100902CO, PIO), and Suomen Kulttuurirahasto (00210970).

Data Availability Statement: Not applicable.

Conflicts of Interest: The authors declare no conflict of interest.

References

1. European Union, P.O. of the E. Masterplan for a Competitive Transformation of EU Energy-Intensive Industries Enabling a Climate-Neutral, Circular Economy by 2050. Available online: http://op.europa.eu/en/publication-detail/-/publication/be308ba7-14da-11ea-8c1f-01aa75ed71a1 (accessed on 21 December 2021).
2. International Energy Agency *Renewables 2018: Analysis and Forecasts to 2023.*; 2018; ISBN 978-92-64-30684-4.
3. Vargas, F.; Domínguez, E.; Vila, C.; Rodríguez, A.; Garrote, G. Agricultural Residue Valorization Using a Hydrothermal Process for Second Generation Bioethanol and Oligosaccharides Production. *Bioresource Technology* **2015**, *191*, 263–270, doi:10.1016/j.biortech.2015.05.035.
4. Toor, M.; Kumar, S.S.; Malyan, S.K.; Bishnoi, N.R.; Mathimani, T.; Rajendran, K.; Pugazhendhi, A. An Overview on Bioethanol Production from Lignocellulosic Feedstocks. *Chemosphere* **2020**, *242*, 125080, doi:10.1016/j.chemosphere.2019.125080.
5. Gallone, B.; Mertens, S.; Gordon, J.L.; Maere, S.; Verstrepen, K.J.; Steensels, J. Origins, Evolution, Domestication and Diversity of Saccharomyces Beer Yeasts. *Current Opinion in Biotechnology* **2018**, *49*, 148–155, doi:10.1016/j.copbio.2017.08.005.
6. Takada, M.; Chandra, R.; Wu, J.; Saddler, J.N. The Influence of Lignin on the Effectiveness of Using a Chemithermomechanical Pulping Based Process to Pretreat Softwood Chips and Pellets Prior to Enzymatic Hydrolysis. *Bioresource Technology* **2020**, *302*, 122895, doi:10.1016/j.biortech.2020.122895.
7. *Biofuels, Solar and Wind as Renewable Energy Systems: Benefits and Risks*; Pimentel, D., Ed.; Springer: Dordrecht, 2008; ISBN 978-1-4020-8653-3.
8. McCaherty, J.; Wilson, C.; Cooper, G. 2019 ETHANOL INDUSTRY OUTLOOK - Renewable Fuels Association. **2019**.
9. Liu, C.-G.; Xiao, Y.; Xia, X.-X.; Zhao, X.-Q.; Peng, L.; Srinophakun, P.; Bai, F.-W. Cellulosic Ethanol Production: Progress, Challenges and Strategies for Solutions. *Biotechnology Advances* **2019**, *37*, 491–504, doi:10.1016/j.biotechadv.2019.03.002.
10. Vu, H.P.; Nguyen, L.N.; Vu, M.T.; Johir, M.A.H.; McLaughlan, R.; Nghiem, L.D. A Comprehensive Review on the Framework to Valorise Lignocellulosic Biomass as Biorefinery Feedstocks. *Science of The Total Environment* **2020**, *743*, 140630, doi:10.1016/j.scitotenv.2020.140630.

11. López-Gómez, J.P.; Pérez-Rivero, C.; Venus, J. Valorisation of Solid Biowastes: The Lactic Acid Alternative. *Process Biochemistry* **2020**, *99*, 222–235, doi:10.1016/j.procbio.2020.08.029.
12. Ahmed, I.N.; Yang, X.-L.; Dubale, A.A.; Shao, R.; Guan, R.-F.; Meng, X.; Xie, M.-H. Zirconium Based Metal-Organic Framework in-Situ Assisted Hydrothermal Pretreatment and Enzymatic Hydrolysis of Platanus X Acerifolia Exfoliating Bark for Bioethanol Production. *Bioresource Technology* **2019**, *280*, 213–221, doi:10.1016/j.biortech.2019.02.041.
13. Lee, C.S.; Conradie, A.V.; Lester, E. Review of Supercritical Water Gasification with Lignocellulosic Real Biomass as the Feedstocks: Process Parameters, Biomass Composition, Catalyst Development, Reactor Design and Its Challenges. *Chemical Engineering Journal* **2021**, *415*, 128837, doi:10.1016/j.cej.2021.128837.
14. Alves-Ferreira, J.; Lourenço, A.; Morgado, F.; Duarte, L.C.; Roseiro, L.B.; Fernandes, M.C.; Pereira, H.; Carvalheiro, F. Delignification of Cistus Ladanifer Biomass by Organosolv and Alkali Processes. *Energies* **2021**, *14*, 1127, doi:10.3390/en14041127.
15. Eades, P.; Kusch-Brandt, S.; Heaven, S.; Banks, C.J. Estimating the Generation of Garden Waste in England and the Differences between Rural and Urban Areas. *Resources* **2020**, *9*, 8, doi:10.3390/resources9010008.
16. Karimi, S.; Karimi, K. Efficient Ethanol Production from Kitchen and Garden Wastes and Biogas from the Residues. *Journal of Cleaner Production* **2018**, *187*, 37–45, doi:10.1016/j.jclepro.2018.03.172.
17. Zhang, S.; Wang, Y.; Liu, S. Process Optimization for the Anaerobic Digestion of Poplar (*Populus L* .) Leaves. *Bioengineered* **2020**, *11*, 439–448, doi:10.1080/21655979.2020.1739823.
18. Yu, Q.; Qin, L.; Liu, Y.; Sun, Y.; Xu, H.; Wang, Z.; Yuan, Z. In Situ Deep Eutectic Solvent Pretreatment to Improve Lignin Removal from Garden Wastes and Enhance Production of Bio-Methane and Microbial Lipids. *Bioresource Technology* **2019**, *271*, 210–217, doi:10.1016/j.biortech.2018.09.056.
19. Dessie, W.; Luo, X.; Tang, J.; Tang, W.; Wang, M.; Qin, Z.; Tan, Y. Towards Full Utilization of Biomass Resources: A Case Study on Industrial Hemp Residue and Spent Mushroom Substrate. *Processes* **2021**, *9*, 1200, doi:10.3390/pr9071200.
20. Ciudad Autonoma de Buenos Aires Planta de residuos forestales Available online: https://www.buenosaires.gob.ar/ciudadverde/centro-de-reciclaje/planta-de-residuos-forestales (accessed on 1 March 2022).
21. Aditiya, H.B.; Mahlia, T.M.I.; Chong, W.T.; Nur, H.; Sebayang, A.H. Second Generation Bioethanol Production: A Critical Review. *Renewable and Sustainable Energy Reviews* **2016**, *66*, 631–653, doi:10.1016/j.rser.2016.07.015.
22. Sheng, Y.; Tan, X.; Gu, Y.; Zhou, X.; Tu, M.; Xu, Y. Effect of Ascorbic Acid Assisted Dilute Acid Pretreatment on Lignin Removal and Enzyme Digestibility of Agricultural Residues. *Renewable Energy* **2021**, *163*, 732–739, doi:10.1016/j.renene.2020.08.135.
23. Muaaz-Us-Salam, S.; Cleall, P.J.; Harbottle, M.J. Application of Enzymatic and Bacterial Biodelignification Systems for Enhanced Breakdown of Model Lignocellulosic Wastes. *Science of The Total Environment* **2020**, *728*, 138741, doi:10.1016/j.scitotenv.2020.138741.
24. Jimenez-Gutierrez, J.M. (Chema); Verlinden, R.A.J.; van der Meer, P.C.; van der Wielen, L.A.M.; Straathof, A.J.J. Liquid Hot Water Pretreatment of Lignocellulosic Biomass at Lab and Pilot Scale. *Processes* **2021**, *9*, 1518, doi:10.3390/pr9091518.
25. Song, Y.; Cho, E.J.; Park, C.S.; Oh, C.H.; Park, B.-J.; Bae, H.-J. A Strategy for Sequential Fermentation by Saccharomyces Cerevisiae and Pichia Stipitis in Bioethanol Production from Hardwoods. *Renewable Energy* **2019**, *139*, 1281–1289, doi:10.1016/j.renene.2019.03.032.
26. Mota, T.R.; Oliveira, D.M.; Morais, G.R.; Marchiosi, R.; Buckeridge, M.S.; Ferrarese-Filho, O.; dos Santos, W.D. Hydrogen Peroxide-Acetic Acid Pretreatment Increases the Saccharification and Enzyme Adsorption on Lignocellulose. *Industrial Crops and Products* **2019**, *140*, 111657, doi:10.1016/j.indcrop.2019.111657.
27. Wi, S.G.; Cho, E.J.; Lee, D.-S.; Lee, S.J.; Lee, Y.J.; Bae, H.-J. Lignocellulose Conversion for Biofuel: A New Pretreatment Greatly Improves Downstream Biocatalytic Hydrolysis of Various Lignocellulosic Materials. *Biotechnol Biofuels* **2015**, *8*, 228, doi:10.1186/s13068-015-0419-4.

28. Ghavami, N.; Özdenkçi, K.; Salierno, G.; Björklund-Sänkiaho, M.; De Blasio, C. Analysis of Operational Issues in Hydrothermal Liquefaction and Supercritical Water Gasification Processes: A Review. *Biomass Conv. Bioref.* **2021**, doi:10.1007/s13399-021-02176-4.
29. Roman, J.; Neri, W.; Fierro, V.; Celzard, A.; Bentaleb, A.; Ly, I.; Zhong, J.; Derré, A.; Poulin, P. Lignin-Graphene Oxide Inks for 3D Printing of Graphitic Materials with Tunable Density. *Nano Today* **2020**, *33*, 100881, doi:10.1016/j.nantod.2020.100881.
30. Liu, C.; Li, M.; Mei, C.; Chen, W.; Han, J.; Yue, Y.; Ren, S.; French, A.D.; Aita, G.M.; Eggleston, G.; et al. Cellulose Nanofibers from Rapidly Microwave-Delignified Energy Cane Bagasse and Their Application in Drilling Fluids as Rheology and Filtration Modifiers. *Industrial Crops and Products* **2020**, *150*, 112378, doi:10.1016/j.indcrop.2020.112378.
31. Louis, A.C.F.; Venkatachalam, S. Energy Efficient Process for Valorization of Corn Cob as a Source for Nanocrystalline Cellulose and Hemicellulose Production. *International Journal of Biological Macromolecules* **2020**, *163*, 260–269, doi:10.1016/j.ijbiomac.2020.06.276.
32. Taşar, Ş.; Özer, A. A Comparative Study of Hemicellulose Isolation with Hot Water, Alkaline, and Delignification Methods from Tea Leaf Brewing Waste. *Biomass Conv. Bioref.* **2020**, doi:10.1007/s13399-020-00978-6.
33. Otalora, C.M.; Bonifazi, E.; Fissore, E.N.; Basanta, F.; Gerschenson, L.N. Thermal Stability of Betalains in By-Products of the Blanching and Cutting of Beta Vulgaris L. Var Conditiva. *Pol. J. Food Nutr. Sci.* **2020**, *70*, 15–24, doi:10.31883/pjfns/116415.
34. Hernández, Y.R.; García Serrano, L.A.; Maruri, D.T.; Jiménez Aparicio, A.R.; Camacho Díaz, B.H.; Arenas Ocampo, M.L. Optimization of the Microwave-Assisted Ethanosolv Extraction of Lignocellulosic Compounds from the Bagasse of Agave Angustifolia Haw Using the Response Methodology. *J. Agric. Food Chem.* **2018**, *66*, 3533–3540, doi:10.1021/acs.jafc.7b04627.
35. Novelli Poisson, G.F.; Juárez, Á.B.; Noseda, D.G.; Ríos de Molina, M.C.; Galvagno, M.A. Adaptive Evolution Strategy to Enhance the Performance of *Scheffersomyces Stipitis* for Industrial Cellulosic Ethanol Production. *Industrial Biotechnology* **2020**, *16*, 281–289, doi:10.1089/ind.2020.0008.
36. Hernández-Hernández, H.M.; Chanona-Pérez, J.J.; Terrés, E.; Vega, A.; Ligero, P.; Farrera-Rebollo, R.R.; Villanueva, S. Microscopy and Spectroscopy Tools for the Description of Delignification. *Cellulose Chemistry and Technology* **2019**, *53*, 87–97.
37. Kus, J. Application of Confocal Laser-Scanning Microscopy (CLSM) to Autofluorescent Organic and Mineral Matter in Peat, Coals and Siliciclastic Sedimentary Rocks — A Qualitative Approach. *International Journal of Coal Geology* **2015**, *137*, 1–18, doi:10.1016/j.coal.2014.10.014.
38. Hernández-Hernández, H.M.; Chanona-Pérez, J.J.; Vega, A.; Ligero, P.; Mendoza-Pérez, J.A.; Calderón-Domínguez, G.; Terrés, E.; Farrera-Rebollo, R.R. Acetosolv Treatment of Fibers from Waste Agave Leaves: Influence of Process Variables and Microstructural Study. *Industrial Crops and Products* **2016**, *86*, 163–172, doi:10.1016/j.indcrop.2016.03.043.
39. Hernández-Hernández, H.M.; Chanona-Pérez, J.J.; Calderón-Domínguez, G.; Perea-Flores, María.J.; Mendoza-Pérez, J.A.; Vega, A.; Ligero, P.; Palacios-González, E.; Farrera-Rebollo, R.R. Evaluation of Agave Fiber Delignification by Means of Microscopy Techniques and Image Analysis. *Microsc Microanal* **2014**, *20*, 1436–1446, doi:10.1017/S1431927614012987.
40. Savic, I.M.; Savic Gajic, I.M. Optimization Study on Extraction of Antioxidants from Plum Seeds (Prunus Domestica L.). *Optim Eng* **2021**, *22*, 141–158, doi:10.1007/s11081-020-09565-0.
41. Mukherjee, A.; Banerjee, S.; Halder, G. Parametric Optimization of Delignification of Rice Straw through Central Composite Design Approach towards Application in Grafting. *Journal of Advanced Research* **2018**, *14*, 11–23, doi:10.1016/j.jare.2018.05.004.
42. Montgomery, D.C. *Design and Analysis of Experiments*; Eighth edition.; John Wiley & Sons, Inc: Hoboken, NJ, 2013; ISBN 978-1-118-14692-7.